Wear 486-487 (2021) 204081

Contents lists available at ScienceDirect

Wear

journal homepage: www.elsevier.com/locate/wear

Analysis of the hardness ratio effect on the tribological performance of NiCrBSi coating/debris particles using the Stribeck Curve

K.A. Habib *, D.L. Cano, José Antonio Heredia, J. Serrano-Mira

Department of Industrial System Engineering and Design, Universitat Jaume I, 12071, Castellón, Spain

A R T I C L E I N F O

Keywords:
NiCrBSi coating
Debris
Hardness ratio
Surface roughness
Lubrication regime

A B S T R A C T

This work aims to propose an approach to estimate the final surface roughness as a function of the hardness ratio between coating and debris ($H_{pin}/H_{debris} = H_p/H_d$) under lubricated conditions employing pin-on-disc configuration. Using this approach provides a better understanding and prediction of the lubrication regime (Stribeck Curve) compared with the traditional approach that uses the initial surface roughness. Our results demonstrate that a lower hardness ratio induces a higher friction coefficient and contributes to a marked increase in wear rate in lubricated conditions. To find an effective method for simulating the debris effect, four types of NiCrBSi powders were used as a source of debris: two metallic powders with a completely spherical morphology but different Cr concentrations and two other NiCrBSi (15.25%Cr) powders mixed with different concentrations 40 and 60% of ceramic, Zr + 7% Y_2O_3 (ZSP), composed of spherical particles morphology. Therefore, a set of four sources of debris material specimens were simulated by different types of particles with a similar size distribution but different average hardness. Each of these particles was dispersed in an oil lubricant. Observation of the worn surfaces using a rugosimeter and scanning electron microscope suggested that, together with the shape, size and number of debris, the hardness ratio must be considered when studying the tribological behavior of machine components. The proposed methodology may help to predict the variation in lubrication regime parameters (Stribeck curve) by controlling the hardness ratio.

1. Introduction

The presence of solid particles contaminating lubricants is a persistent problem and the most harmful form of contamination in industrial settings affecting the performance and reliability of machinery components such as bearings, axles, valves, gears, engine pistons, dynamic seals, and in tribosystems in which abrasion is the predominant wear mechanism. Chutes, hydraulic systems with dirt, extruders, rock crushers, dies in powder metallurgy and slides in which the surface of the counterbody exhibits protuberances or embedded hard particles are components which may suffer wear due to abrasion. Different physical processes may be involved in abrasion, depending on the wearing materials and operating conditions such as the type of abrasive particles, attack angle, etc. [1]. These components are normally operating in the presence of thousand to millions of particulates in their intimate environment with different size ranges, shape, morphology, and hardness [2]. The presence of suspended debris particles in the lubricating oil shown to be a major problem in many industries, manufacturing processes and an important factor affecting the long-term survival of the machinery components; it can be indicative of potential machine faults and may cause catastrophic component failure during operation [3]. So many industrial failures are in fact related to lubricant contaminates and probably are the most frequent causes of failures of machinery elements, yet it is an area that has not always been given the appropriate level of attention.

The formation of debris particles is due to the abrasion, adhesion and the introduction of particles from the environment, such as soot due to incomplete combustion [4]. Although frequent oil change and filtration may ameliorate the effects, it is impossible to avoid completely the presence of debris. It is convenient to know how the different types of debris affect wear to select the appropriate lubricant additives and surface treatments [5]. The presence of debris particles in sliding clearance contacts of machinery components is often detrimental at both the microscale and nanoscale, since it can increase friction, induce indentation abrasive wear, reduce actual lubricant film thickness and compromise the lubrication performance [6]. It is generally recognized that friction coefficient and the degree of wearing surface damage depends on the debris concentration, hardness, size and morphology [7,8]

* Corresponding author.
E-mail address: razzaq@esid.uji.es (K.A. Habib).

https://doi.org/10.1016/j.wear.2021.204081
Received 29 April 2021; Received in revised form 18 August 2021; Accepted 23 August 2021
Available online 27 August 2021

although quantitative studies are rare.

Most machinery components work under lubricated conditions, where the lubricant plays an important aspect in the performance of the tribo-pair by reducing the friction coefficient and lengthening the service life. Specifically, under boundary as well as mixed lubrication regimes, the chemical characteristics of oil and additives and the oxygen concentration in the environment will decide the tribological behaviour of the contact surfaces [9].

Many publications have shown experimentally the detrimental influence of debris particles in machine-elements operation, such effects include increase of friction coefficient and temperature [10,11], dramatic increase of wear even by soft particle debris [12,13], increase of vibration and noise [14,15] and substantial decrease of component fatigue life [16–18]. Several studies have focused on the mechanism of surface indentation from two points of view: theoretically via elementary stress analysis [19,20] via finite-elements [21,22] and experimentally [8,23].

In the light of current literature on fundamental abrasive wear, it is worth highlighting the studies concerning debris induced damage authored by Grieve, DG, Dwyer-Joyce [24], Nilsson, R, Dwyer-Joyce [25] and Underwood, RJ [26]. Previous studies have shown how increasing in the debris particle size contributes to a significant increase in the friction coefficient and wear rates and may alter the lubrication regime [27] and how the damage mechanisms are related to the particle size [28].

Although most studies (such as D.A.Rigney [29], P.J.Firkins et al. [30], G. Straffelini et al. [31] and Trevisiol et al. [32] show that hardness is one of the key factors which influence the sliding behavior of different materials combination, there is a lack of research on its mechanisms [7]. Therefore, tribological studies are becoming increasingly needed in the understanding of mechanisms of friction, wear, and lubrication in the presence of debris particles with different hardness and studying the effect of counterpart surface hardness.

Accordingly, the present investigation has aimed to conduct experiments with two objectives in mind: first, to study the effect of debris, with approximately similar sizes but different hardness dispersed in an oil lubricant in relation with the pin coating hardness ($H_{pin}/H_{debris} = H_p/H_d$), on the friction coefficient and wear behavior of the surfaces under lubricated conditions; and second, to propose a general approach to empirically develop predictions of surface damage caused by debris particles with different hardness and the evolution of lubrication regime according to the hardness ratio H_p/H_d (surface hardness in relation with debris particles hardness).

In this study, we test NiCrBSi coatings as one of the alloys that provide better performance in a variety of industrial sectors [33]. NiCrBSi coatings are manufactured by a conventional thermal deposition process, oxy-fuel (OF) followed by Surface Flame Melting (SFM) process. The technique displays a sequence of unique and interesting properties such as a lamellar splats structure, high density, low porosity, in-flight oxidation of sprayed particles, adhesion strength, high tensile strength, outstanding thermal and dimensional stability, oxidation resistance and low heat transfer to the substrate [34]. Thermally sprayed Ni-based coatings are frequently used in applications where wear and corrosion resistance at atmospheric, moderate and elevated temperatures are required [35,36]. Different NiCrBSi (15.25% Cr) combined with ZSP + 7% Y_2O_3 powders are used to manufacture the experimental coating in order to generate particles of different hardness during the tribology tests. A pin-on-disc friction and nanoindentation measurements are conducted to relate the friction coefficient with the lubricated regime in each case. The topography and morphology of the surfaces are studied to understand their appearance and to study the wear behavior. And finally, the results are expressed quantitatively by fitted equations.

2. Experimental procedure

2.1. Materials

In accordance with the ASTM G 99 standard, cylindrical pins were cut from AISI 304 stainless steel bars. The pins were 18 mm in length and 8 mm in diameter. One end of the cylindrical pin was coated with self-fluxing NiCrBSi (commercially available powder, Amperit M-772.33) with the following chemical composition (in wt.%): 0.3 C, 3.52 Si, 1.7 B, 7.71 Cr, 2.66 Fe, and balance Ni, with a microhardness of approximately 361 HV_{200gf} after thermal deposition. Fig. 1 shows the morphology of the powder, which was used for the pin coating. The counterpart disc for pin-on-disc tribology test used for this investigation was hardened and tempered F-5220 (100 mm diameter and 5 mm thickness) in line with A68a (01) with average microhardness of 930 HV_{200gf}, in order to reduce the effect of debris particles on the disc and to only investigate its effect on NiCrBSi pin coatings.

In order to obtain correlation between NiCrBSi initial pin coating hardness and initial debris hardness, several kinds of both metallic (Eutalloy PE 3307 with the following chemical composition, (in wt.%): 0.4 C, 3.1 Si, 1.6 B, 10.1 Cr, Fe 2.8, Ni 81.94, Eutalloy PE 3309 (in wt.%): 0.4 C, 3.1 Si, 1.6 B, 15.25 Cr, Fe 2.8, Ni 76.04) and Metal Matrix Composites (MMC) materials (cermet's) (Eutalloy PE 3309 + 40% partially stabilized zirconia ceramics ZrO_2 + 7% Y_2O_3 (ZSP) and PE 3309 + 60% ZSP) powder materials with a completely spherical morphology and with a range of hardness, from soft to very hard (harder than the pin coating), were used as debris source in the present investigation. These particles were dispersed in lubricated oil. The hardness and particle size of the powders used as debris sources (made by Castolin Eutectic and the ceramics are made by PRAXAIR) are shown in Table 1.

The source of debris particles used in this study generally had a spherical morphology, as shown in Fig. 2.

2.2. Thermal deposition process

The coating was deposited onto AISI 304 stainless steel. To improve the adhesion strength of the deposited coating with the substrate, the surface of one end of the pins was grit-blasted with corundum particles (99.6% purity and 0.53 mm mean particle size) prior to the spraying process using an air pressure of 4.5 bar, incidence angle of approximately 90°, and a gun-to-pin distance of 130 mm. The samples were sprayed using a CDS 8000 flame spray torch manufactured by Castolin Eutectic. The thermal spray parameters used to deposit the NiCrBSi coatings are listed in Table 2. Subsequently, the deposited coatings were fused using the surface flame melting (SFM) technique with an oxyacetylene torch at an operating temperature of 1025 °C and a scanning speed of approximately 150 mm/min. To prepare the deposited coating, samples were polished using four sequential steps, namely, 6, 3, and 1 μm grade diamond lapping and 0.05 μm Al_2O_3, and were

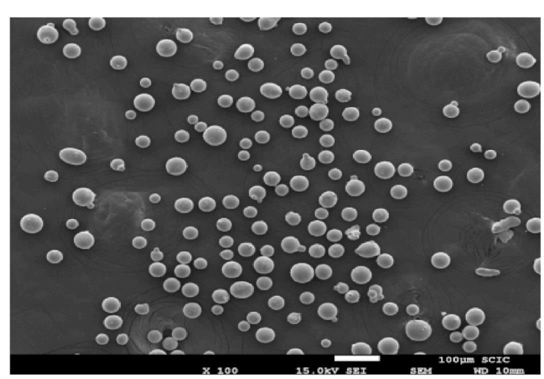

Fig. 1. SEM image showing the initial powder morphology of the NiCrBSi pin coating.

Table 1
Hardness and particle size of debris source.

	NiCrBSi (10.1%Cr)	NiCrBSi (15.25% Cr)	NiCrBSi (15.25%Cr)/ PSZ (60/40%)	NiCrBSi (15.25%Cr)/ PSZ (40/60%)
Designation	Eutalloy PE 3307	Eutalloy PE3309	Eutalloy + PRAXAIR PE 3309 + ZrO 195-2	Eutalloy + PRAXAIR PE 3309 + ZrO 195-2
Hardness HV_{30gf}	330	714	880	1003
Particles size (μm)	125/45	125/45	125/45	125/45

decreased and cleaned with acetone in an ultrasonic bath for 15 min. The surface roughness of the NiCrBSi pin coating was $R_a \approx 0.045$ μm, and the initial surface roughness of the hardened and tempered F-5520 disc was $R_a \approx 0.075$ μm.

2.3. Lubricating oil and tribology tests

The tribological behavior of the NiCrBSi coatings was determined using a tribometer with a pin-on-disc configuration (TE79/P, Plint and Partners) in continuous motion at 25 °C and a humidity of approximately 55%. CUT-MAX 110 mineral oil lubricant with a viscosity of 100 ± 1 cSt and a density of 0.880 g/cm^3. In this work, 2.5 g of powders were used as the debris source, which were mixed thoroughly with 10 ml of test lubricant. The mixture was fed directly onto the contact area of the friction pairs (10 drops per minute). Additionally, particles of the same size and shape have been used to feed approximately the identical amount of abrasive particles per drop of lubricated oil onto the contact area. The tests without the debris particles in lubricant were performed to be as reference to compare with tests with the debris particles in lubricant oil. The parameters of the tribotester were as follows: the apparent pressures were varied between 0.0585, 0.117, 0.175, 0.292, and 0.390 MPa. At each applied pressure, the velocity was increased every 20 m distance in a stepwise manner (0.037, 0.073, 0.110, 0.147, and 0.183 m/s) until the maximum speed of 0.22 m/s. Wear tests were conducted under room temperature and humidity. Self-fluxing NiCrBSi coating over stainless-steel pins was used to analyze the effect of the applied loads and the sliding speeds on the wear rate of the coatings under lubrication conditions against a hardened and tempered F-5220. Several wear tests were performed at different loads (3, 6, 9, 15 and 20 N) at constant sliding speed (0.220 m/s), and at different sliding speed (0.037, 0.073, 0.110, 0.147, 0.183 and 0.22 m/s) whilst the nominal load remained constant at (20 N). Three wear tests were performed for each type of samples, and their results were reproducible within 5% deviation.

3. Results and discussion

3.1. Evaluation of surface topography

The evolution of the surface topography pattern for each of the NiCrBSi pin coatings was measured before and after tribology experiments (after a sliding distance of 600 m under different loads, using particles with different hardness as sources of debris. To obtain quantitative information of surface topography over wear tracks of the specimens, a roughness tester HOMMELWERKE-T8000 was implemented. The surface profile roughness (R_a) was extracted as a line through an area using a stylus rugosimeter. Prior to the profilometry

Table 2
Thermal spray parameters.

Torch speed (mm/s)	Nº of strokes	Distance (mm)	Acetylene pressure (bar)	Oxygen pressure (bar)	Air pressure (bar)	Flame type
67.5	5	130	0.7	4	3	Neutral

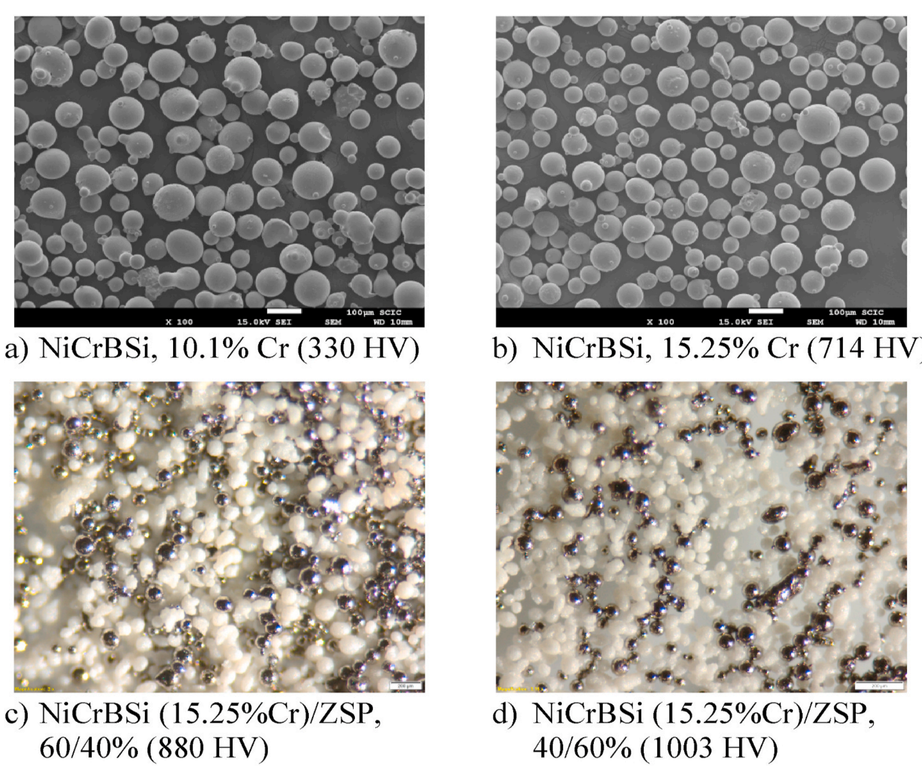

Fig. 2. Powder morphology and hardness of as-received powders used as source of debris. a, b) Metallic NiCrBSi and c, d) cermet's NiCrBSi/ZSP, obtained by SEM (upper) and optical microscopy (lower).

measurements, all samples were ultrasonically cleaned in an acetone bath for 15 min, followed by rinsing with propanol to ensure that they were clean and free from any wear debris and/or residual oil to obtain an accurate measurement of the surface profiles.

The surface topography and roughness of the various specimens were irregular and uneven, with multiple depressions of different depths and widths and waviness spacings that depended on the debris hardness. As shown in Fig. 3, as the surface roughness increased, the surface topography revealed a more marked groove and ridge morphology. The surface roughness values (R_a) ranged from 0.86 to 1.82 μm for the softer and harder particle debris, respectively; while that obtained with just the lubricating oil was as low as 0.075 μm. In addition, Fig. 3 shows that the slope angle of the surface roughness of the NiCrBSi specimens had a direct relation with the debris hardness; a higher slope indicates the occurrence of more roughness features in relation to the roughness profile height. This led to an enlarged specific surface and, therefore, more possibilities for the debris particles to interlock with the NiCrBSi coating. Thus, differences in the debris hardness had a considerable effect on the final surface topography and surface profile roughness (R_a). It is observed from the obtained results shown in Fig. 4 that the average roughness slops angles values are decreased as a function of increase in hardness ratio.

The surface roughness angle slope depends on the forces acting on a debris particle. Fig. 5 shows a shear force F_τ pressing the debris particles trapped in the contact gap. The resulting normal force of debris particles $F_{Nd} = F_{\tau d} \cos \varphi$ or ($\varphi = 90°- \Theta$) and the tangential force $F_{td} = F_{\tau d} \sin \varphi$. An increase in the Θ (angle slop) leads to increase in F_N. Hence, the maximum friction force (μ. F_{Nd}) hindering the debris particles from slipping are increased (where μ is the friction coefficient between the debris particles and NiCrBSi coating). Additionally, F_{td}, which forces the particles debris to slip, is decreased. This may increase the roughness flank micro-deformation.

3.2. SEM worn surface study

The surface morphology of the NiCrBSi pin coatings after 600 m of sliding was investigated using scanning electron microscopy (SEM). It was found that the worn surface of the self-fluxing NiCrBSi pin coating exhibited different roughness parameters and surface topography, which strongly depended on the debris hardness. Fig. 6a shows that the worn surface of the NiCrBSi coating with solely lubricated oil exhibited a flat and smooth surface with numerous randomly scattered pits, tiny dark regions, and a few mild scratch regions, which were probably caused by the accumulation of wear debris particles during friction and wear tests.

As shown in Fig. 6, the hardness and ductility of the debris had a considerable influence on the damage state of the NiCrBSi coating surface acting as a crushing wall against debris. This indicates that the appearance of asperities varied considerably with the debris hardness. When the debris was soft and ductile (NiCrBSi, 10.1% Cr, 330 HV_{30gf}) with a hardness ratio $H_p/H_d = 1.091$, the debris particles may plastically adhere to one another to form large particles. In this case, fewer active cutting debris, large indentations, and craters were made by crushing debris particles, which led to a lower surface roughness (Fig. 6b). In the case of tough debris (NiCrBSi, 15.25%Cr, 714 HV_{30gf}) with a hardness ratio of $H_p/H_d = 0.5$ (Fig. 6c), there were parallel scratches following the direction of the debris movement, which created deeper parallel grooves and irregular surfaces and imparted a relatively higher surface roughness. Finally, when debris particles were hard (Fig. 6d and e) and brittle combined with tough particles (NiCrBSi (15.25%Cr)/ZSP; 60/40% and 40/60%; 880 and 1003 HV_{30gf}, respectively) with hardness ratios $H_p/H_d = 0.41$ and $H_p/H_d = 0.36$, respectively, the brittle particles (ZSP) were successively fractured in the contact area under a certain applied load. Abrasive wear of smaller debris particles tended to produce rough surfaces with significant micro-deformation or noise in the roughness, which was produced by the harder and larger particles embedded in the NiCrBSi coating surface. The occurrence of grooving produced by large particles and rolling abrasion generated by medium-sized particles was observed in both samples, and the surface roughness was highly dependent on the ZSP content.

3.3. Friction coefficient study

Pin-on-disc sliding friction measurements were conducted to determine the effect of the debris hardness on the friction coefficient values of the flame sprayed combined with SFM re-melting NiCrBSi pin against a hardened steel disc. The variation in the friction coefficient with debris hardness ratio for the Ni-based coating is presented in Fig. 7. The variation could begin when the debris particles suspended in the lubricant oil entered between the moving surfaces. Particle debris in contact (larger particles were more likely to be in contact) were subjected to very high pressure, increasing the contact area by both the growth of individual contacts and the initiation of new ones. This pressure generated a deformation process that could take one of three modes depending on the material debris properties and NiCrBSi contact surfaces:

a) The low friction coefficient values for relatively soft and ductile debris (330 HV_{30gf}) and hardness ratio $H_p/H_d = 1.091$ could be attributed to total or partial extrusion or plastification of debris particles into an ellipsoidal shape as they were compressed between the contact surfaces (NiCrBSi coating pin and hardened steel disc) and eventually deformed into a thin platelet. The real contact area was sufficient to support the applied load elastically, resulting in an approximately uniform pressure distribution.
b) For the intermediate friction coefficient values for the tough debris (714 HV_{30gf}) and hardness ratio $H_p/H_d = 0.5$, two possible behaviors may have occurred: 1) particles under certain conditions of load and velocity yielded (elastoplastic or/and plastic deformation) before fracture, and after fracture occurred, the fragments embedded in the NiCrBSi pin coating caused the second phase of the surface damage; 2) debris particles underwent little or no deformation and could embed into the surface of the NiCrBSi pin coating.
c) The higher friction coefficient values corresponding to the harder and brittle debris particles (880 and 1003 HV_{30gf} with 40 and 60% ZSP) and hardness's ratio $H_p/H_d = 0.41$ and $H_p/H_d = 0.36$, respectively, were due to the indentation depth of the debris particles in the NiCrBSi pin coating as well as the indenter shape, size, and hardness. In addition, when brittle debris particles successively fractured in the contact area, their fragments became smaller and smaller as they were crushed [37]. The presence of hard fragments between the sliding surfaces could then embed into the surface of the softer element (NiCrBSi pin coating) or generate an agglomeration of fragmented particles in the surface tracks, which could lead to an increase in the friction coefficient, abrasion, and scuffing. The deformation and/or fracture of debris particles on the contact surface directly affected the friction coefficient and the nature of the damage on the surface of the NiCrBSi pin coating. This particle damage can have a major influence on the friction coefficient and wear rate of moving surfaces.

Therefore, the obtained friction coefficient values were strongly dependent on the hardness ratio. Fig. 7, depicts the variation in the friction coefficient with the hardness ratio H_p/H_d for the NiCrBSi coating and the different powders used as a source of debris. It consists of two straight sections. In the first section, the friction coefficient rises minimally (markedly low slope with a narrow range of variation) from 0.155 to 0.170, when the hardness ratio changes from $H_c/H_p = 1.091$ to $H_p/H_d = 0.5$ (wide variation in the hardness ratio). In contrast, the second section has a rapid and significant increase (sharp slope or wide range of variation) in the friction coefficient values from 0.170 to 0.203 to 0.226, and the hardness ratio changes from $H_p/H_d = 0.5$ to 0.41 and 0.36

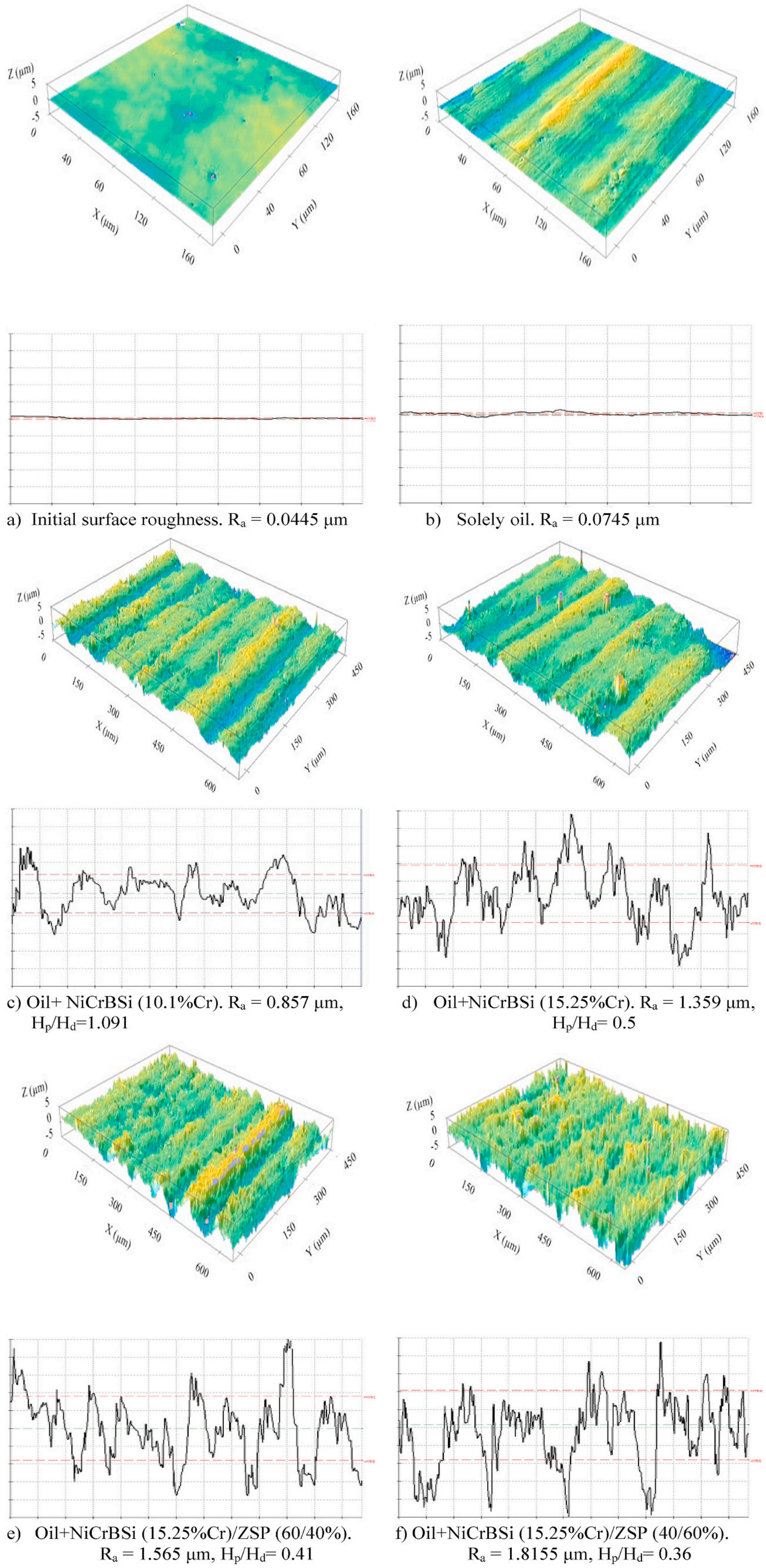

a) Initial surface roughness. R_a = 0.0445 µm

b) Solely oil. R_a = 0.0745 µm

c) Oil+ NiCrBSi (10.1%Cr). R_a = 0.857 µm, H_p/H_d=1.091

d) Oil+NiCrBSi (15.25%Cr). R_a = 1.359 µm, H_p/H_d= 0.5

e) Oil+NiCrBSi (15.25%Cr)/ZSP (60/40%). R_a = 1.565 µm, H_p/H_d= 0.41

f) Oil+NiCrBSi (15.25%Cr)/ZSP (40/60%). R_a = 1.8155 µm, H_p/H_d= 0.36

Fig. 3. 3-D geometric morphology and 2-D surface profiles of NiCrBSi coatings after 600 m distance.

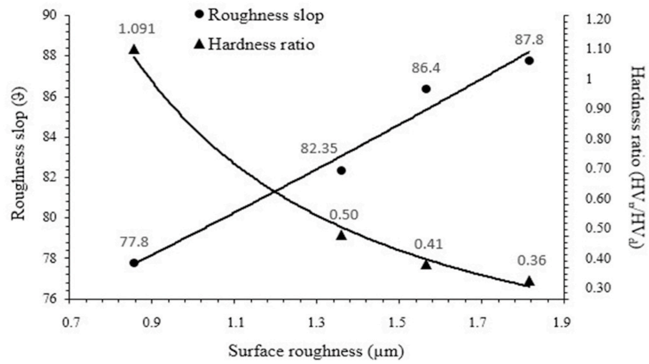

Fig. 4. Relationship between surface roughness, debris hardness ratio and average surface roughness slope angles.

(narrow hardness ratio range), respectively.

3.4. Nano-indentation study

The evolution of the mechanical properties of NiCrBSi coatings after 600 m of sliding distance by means of work hardening (i.e., strain hardening) was studied using a fully calibrated Nano indenter G-200 equipped with the ultralow load and ultra-high resolution Dynamic Contact Module (DCM), which was made by Keysight (formerly Agilent), using a Berkovich indenter pit. Basic nanoindentations were determined by controlling the maximum depth to 2 μm. At least 25 measurements were taken in different zones, and the average values were considered in this work. It was evident that strain hardening occurred during the wear process for the NiCrBSi specimens, and the results are presented in Table 3. The increase in the nanoindentation values in the wear scars is further evidence of the extensive plastic deformation, and the higher nanoindentation values corresponded to lower hardness ratio.

3.5. Relating the hardness ratio with the lubrication regime parameters

The well-known Stribeck curve describes the behavior of the friction coefficient as a function of the so-called Hersey number, which is a key parameter in this curve. The viscosity and speed over the applied load parameter can be interpreted as the lubricant film thickness. The inclusion of R_a, the initial surface roughness, in this parameter was proposed by Schipper, which is defined as $Z = \eta \cdot \nu / p_a \cdot R_a$ [38–40]. Previous work [27] showed that using the actual surface roughness estimated as a function of debris particle size allows a better determination and prediction of the lubrication regime for the wear process compared with the traditional approach that uses the initial surface roughness. In this paper, the results of a series of experiments performed with pin-on-disc tests are reported together with a theoretical and practical prediction of the Stribeck-type behavior. Various loads and velocities were considered to determine the effect of the hardness ratio of the NiCrBSi pin coating and the source of debris with various hardness values. The final surface roughness was considered variable in this study, which was highly dependent on the hardness ratio; therefore, the abscissa values (R_{af}) were used. Moreover, all the experimental results indicate that the effect of the debris hardness became more dominant with increasing sliding distance, suggesting that the particle hardness had an adverse effect on the surface roughness with sliding distance. Fig. 8 shows the predicted Stribrck curves of the reference NiCrBSi pin/steel disc contact with solely oil and NiCrBSi pin coating against debris with different hardness ratios after 600 m of sliding distance. The λ value of the tribosystem in this work, as a function of friction coefficient corresponding to the BL and ML is about (0.9–2.7) respectively, where the minimum oil film was calculated based on the Hamrock-Dowson equation for lubricated elliptical contacts [41,42].

To better understand the evolution of the surface morphology and roughness profile of the NiCrBSi pin coating after 600 m of sliding, two key parameters must be considered: the hardness ratio of the contact surface (NiCrBSi coating) to each debris hardness (H_p/H_d) and the surface roughness. Fig. 9 demonstrates that a higher hardness ratio resulted in lower surface roughness, and vice versa.

In maintenance operation and some applications, it would be difficult to directly measure the final surface roughness. Therefore, it would be useful to find a relationship between the debris hardness, which can be determined by nanoindentations using indenters with different shapes, such as Berkovich and cylindrical indenters or with non-contact atomic force microscopy (AFM) nanoindentation as a method to determine nanoindentation of particles debris [43,44], during maintenance operations, and the surface roughness estimation. The relationship between the hardness ratio and the surface roughness can be fitted according to the following equation:

$$R_{af} = K \left(\frac{H_p}{H_d}\right)^{-n} \tag{1}$$

In this relationship, the exponent (-n) represents how the two variables (H_p/H_d and R_{af}) are related, while the K coefficient simply amplifies or reduces the value obtained for R_{af} without altering the relationship between R_{af} and H_p/H_d.

For this study, the equation fitted with experimental data is:

$$R_{af} = 0.8981 \left(\frac{H_p}{H_d}\right)^{-0.649} \tag{2}$$

It has been observed that there is a good correlation between the debris hardness and Stribeck parameters. To be more precise, we proposed another method to assess the Stribeck curve parameters by determining the relationship between the hardness of the NiCrBSi coating and debris particle hardness (H_p/H_d). Therefore, this study proposes to incorporate the hardness ratio (H_p/H_d) into the lubricant

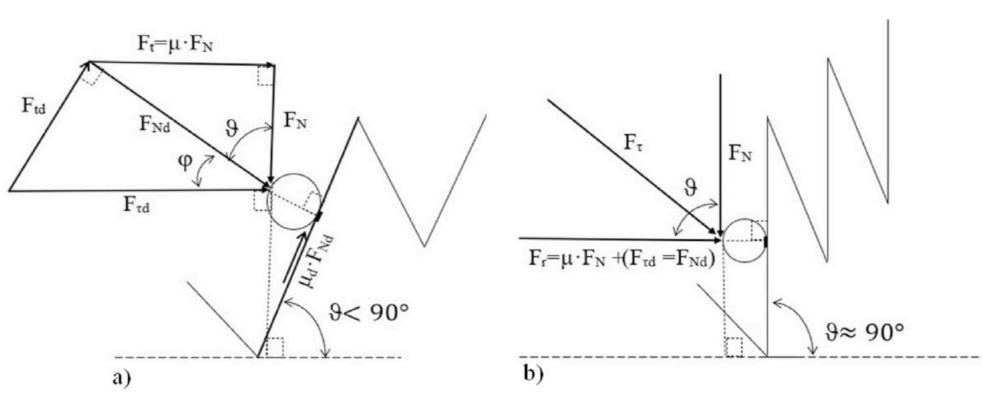

Fig. 5. Forces acting on the debris particles: a) when the slope angle is lower than 90° and b) when $F_{rd} = F_{Nd}$.

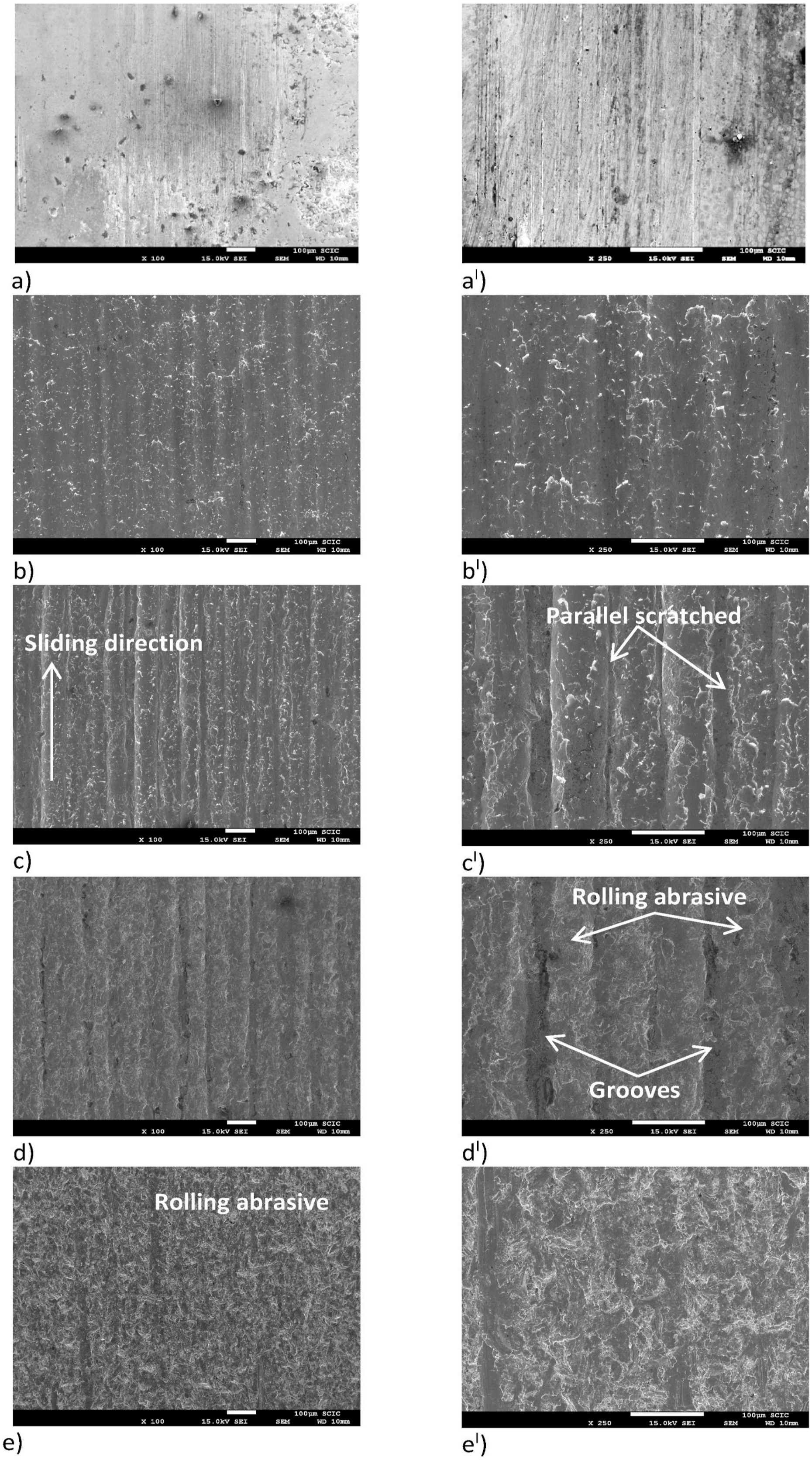

Fig. 6. SEM image of surface morphology at different magnification; a) solely oil, b) lubricant oil + NiCrBSi (10.1%Cr) ($H_p/H_d = 1.091$), c) lubricant oil + NiCrBSi (15.25%Cr) ($H_p/H_d = 0.5$), d) Oil + NiCrBSi (15.25%Cr)/ZSP, 60/40%) ($H_p/H_d = 0.41$) and e) Oil + NiCrBSi (15.25%Cr)/ZSP, 40/60%) ($H_p/H_d = 0.36$).

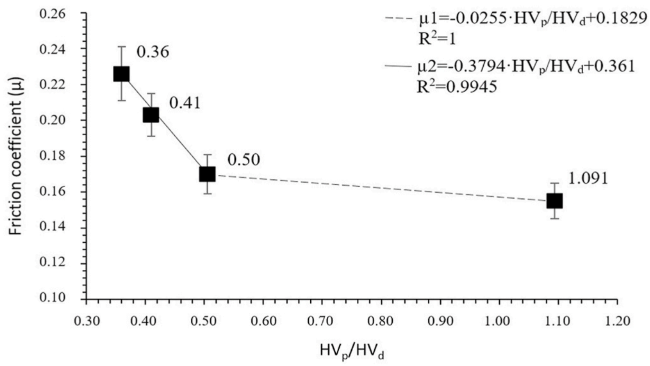

Fig. 7. Dependence of friction coefficient on the hardness ratio.

Table 3
The dependence between the degree of hardening values of NiCrBSi coating with different debris hardness after 600 m distance.

	Solely oil	Oil+330 HV_{30gf}	Oil+714 HV_{30gf}	Oil+880 HV_{30gf}	Oil+1003 HV_{30gf}
Nanoindentation (GPa)	4.55	5.01	5.7	7.2	8.18
Modulus of elasticity, E (GPa)	174.6	191.8	198.3	237.5	270.5

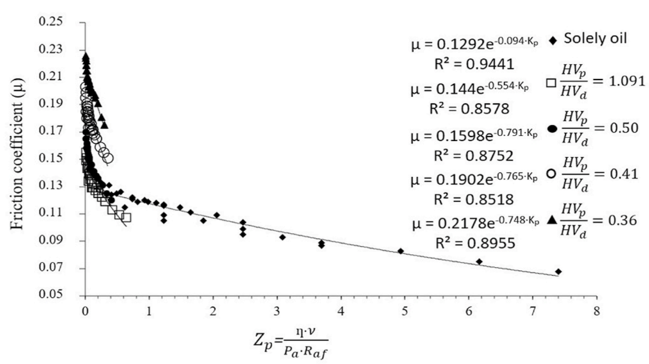

Fig. 8. Stribeck curves for the NiCrBSi coating sliding against debris with various hardness ratios after 600 m of sliding.

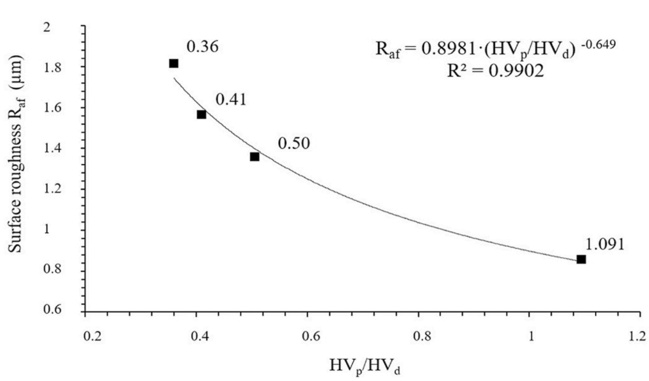

Fig. 9. Variation of surface roughness as a function of hardness ratio H_p/H_d.

number of Schipper in place of the initial surface roughness. By including this fitted equation (Eq. (2)) in the expression for the lubrication parameters (lubrication number, Z), the following expression was obtained:

$$K_L = \eta \cdot v \Big/ P_a \, 0.8981 \left(\frac{H_p}{H_d}\right)^{-0.649} \tag{3}$$

The effect of including the final surface roughness (R_{af}) after 600 m distance in the Hersey number for the NiCrBSi coatings can be illustrated by Stribeck curve. Using the new lubrication number (K_L), the Stribeck curve for NiCrBSi coating contacts with different debris hardness ratio is shown in Fig. 10. The results indicate that all the Stribeck-like curves exhibited an exponential tendency; therefore, two lubrication regimes (boundary and mixed) can be easily distinguished by each curve but with different slopes and different lubrication numbers (Table 4). It can be seen that a decreasing of hadness ratio (H_p/H_d) leads to shifting of the lubrication number (K_L) value to left where much sever contact conditions are realized.

3.6. Wear behavior

The wear tests were run for each of the specified test conditions during which the NiCrBSi coatings weight loss was measured every 120 m up to a total distance of 600 m. The wear rate is calculated with a modified Archard equation reported by Hutchings and Shipway [45] (k = W/LC), where: W = wear in cm^3, L = sliding length in m, C = normal load in N, can be used to calculate the wear rate coefficient k in cm^3/Nm. The total volume worn away, can be calculated using equation (ρ = M/V) where ρ is the coating density (7089 kg/m^3) [46] and M the total weight loss during each test. The loss of material was determined by weighting the samples before and after 120 m for each load and different velocities, and ultrasonic cleaning was carried out for each of them. The total sliding distance was almost 600 m. The study uses soft and highly abrasive particles to simulate the favorable and most unfavorable conditions under which the debris has greater hardness than the NiCrBSi pin coating. To better understand the wear mechanism for each coating, one needs to consider the hardness of both the NiCrBSi pin coating and debris particles with different hardness. And in order to make it more comprehensive, it is essential to take at least three key parameters in consideration: the influence of hardness ratio of the contact surface (coating) to debris particles surface (H_p/H_d) on the surface roughness and therefore its effect on the lubrication regimes.

The results of studying the 3-D geometric morphology and 2-D surface profiles of NiCrBSi coatings after 600 m distance (Fig. 3), agree with the analysis of wear surface morphology with SEM (Figs. 11 and 12). Fig. 11 shows SEM images of the NiCrBSi pin coatings after a sliding distance of 600 m with various test conditions: solely oil, oil +2.5 g NiCrBSi (10.1%Cr), oil + 2.5 g NiCrBSi (15.25%Cr), oil+2.5 g NiCrBSi (15.25%Cr/ZSP, 60/40%), and oil+2.5 g NiCrBSi (15.25%Cr/ZSP, 40/60%). The worn surface of the NiCrBSi pin coating with solely oil, used as a reference test, generally displayed a smooth crater wear region, lower plastic flow, and dispersed points of adhesion as could be observed in Fig. 11. The adhesive junctions result in attractive forces between NiCBSi pins coating and hard disc in local close contact were fractured

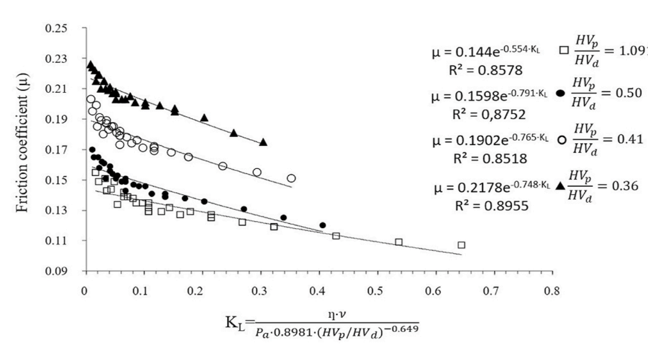

Fig. 10. The effect of new lubrication number (K_L) on friction coefficient for the NiCrBSi coating sliding against different debris hardness ratio.

Table 4
Parameters of Stribeck curve for each hardness ratio H_p/H_d after 600 m tests distance.

	μ_{max}	μ_{min}	K_{Lmax}	K_{Lmin}	R_{af} (μm)	H_p/H_d
Solely oil	0.138	0.068	7.3983	0.1850	0.0745	–
NiCrBSi. 10.1%Cr (330 HV_{30gf})	0.155	0.107	0.6431	0.0161	0.857	1.091
NiCrBSi. 15.25%Cr (714 HV_{30gf})	0.17	0.12	0.4056	0.0101	1.359	0.5
NiCrBSi/(15.25%Cr)/ ZSP. 60/40% (880 HV_{30gf})	0.203	0.151	0.3522	0.0088	1.565	0.41
NiCrBSi(15.25%Cr)/ ZSP. 40/60% (1003 HV_{30gf})	0.226	0.175	0.3037	0.0076	1.815	0.36

under shear stress and further caused the generation of wear debris. This process is favored by plastic deformation and cleanliness associated with changes in the near surface microstructure [47,48]. This may result in detachment or material transfer from NiCrBSi pin coating surface to the hard disc. The fine grooves on the worn surface indicate micro-cutting wear of the surface coating caused by the counterpart hard disc; therefore, the main wear mechanisms of the NiCrBSi coating were micro-cuttings, but scattered adhesive points also take place.

Fig. 12a shows the case of soft and ductile debris (330 HV_{30gf}) and hardness ratios $H_p/H_d = 1.091$. The worn surface exhibited a mild parallel scratch with comparatively lower plastic flow and hence wears rates, which was caused by the sliding of extruded debris particles or the rolling of partially deformed particles. Fig. 12b shows deep parallel scratches of different widths with plastically deformed edges, plough, and pull-out zones, which were caused by the tough NiCrBSi (15.25%Cr) particles (714 HV_{30gf}) with a hardness ratio of $H_p/H_d = 0.5$, and the dominant wear mechanisms of the pin coating were abrasive and cohesive wear (between NiCrBSi pin coating and harder particles debris) with a plastic deformation process. This suggests that grooves are formed by the debris particles and not by asperities of counterpart hard disc. As seen in Fig. 5, the penetration of a sliding abrasive particle into a metallic surface results in micro-ploughing or micro-cutting depending on the angle of attack. Sliding of hard debris particles on NiCrBSi coating of less hardness can undergoes mainly elastic-plastic deformations depending on the angle of attack [1,48].

Typical wear craters were produced on the surface of the NiCrBSi (15.25%Cr) + 40% ZSP coating due to the use of debris with a hardness of 880 HV_{30gf} and hardness ratio of $H_p/H_d = 0.41$. Details of the wear mechanisms within the wear crater were obtained using SEM (Fig. 12c and c^I). The variation in the hardness ratio induced changes in the wear micromechanisms. Grooving was clear within the wear craters, indicating sliding of the abrasive particle debris. The use of the mixture formed by NiCrBSi (15.25%Cr) + 40% ZSP led to the occurrence of multiple indentations, rolling abrasion, plastic deformation, and micro-scratching. A mixed abrasion (rolling abrasion and cutting) regime was observed in this case. When the source of debris was composed of a mixture of metallic particles (NiCrBSi (15.25%Cr) and 60% ZSP with 1003 HV_{30gf} and hardness ratio $H_p/H_d = 0.36$), the worn surface of the NiCrBSi pin coating revealed a considerable amount of plastic flow, scars, grooving abrasion, and micro-blowing severe indentation, and the rolling abrasion mechanism was found to be dominant at a lower hardness ratio (H_p/H_d). This process occurred when a significant proportion of ZSP particles were embedded in the surface of the NiCrBSi coating and acted as indenters, producing a series of fine grooves on the specimen surface, as shown in Fig. 12d and d^I. The weight loss of the flame-sprayed NiCrBSi coatings was determined by the extent of penetration of abrasive particles and damage caused by grooving, cutting and plowing material removal mechanisms as well as plastic flow. The wider groove in the NiCrBSi coatings was due to lack of lubrication and lower hardness relative to the debris particle hardness. Because of the low hardness ratio, the depth of penetration of abrasive particles increased, resulting in increased wear rate of the coatings [49].

So, the interaction between debris particles and NiCrBSi pins coating can govern the fact that the debris can roll, especially at lower loads. The roll-like wear debris are created by two bodies. Each roll is subjected to opposing tangential forces at its top and bottom surfaces. The torque resulting from these forces causes the debris to roll. The axes of roll debris particles are aligned perpendicularly to the sliding direction, indicating that they were rolling on the wear track, and suggesting that the debris particle circulation is common in the contact.

Three tests were performed for each of the specified test conditions, during which the NiCrBSi pins coatings weight loss was measured every 120 m up to a total distance of 600 m. It was found that increasing the hardness ratio from 0.36 to 0.41 decreases the mass loss of the NiCrBSi coating (53% ± 1.118%), from 0.41 to 0.51 reduces the mass loss (28.57% ± 0.761%) and finally from 0.51 to 1.091 considerably reduces the accumulative mass loss (86.36% ± 0.313%). These results demonstrated that the hardness ratio H_p/H_d values produced a significant effect on mass loss of NiCrBSi coatings, Fig. 13.

Fig. 14, shows that when the value H_p/H_d is less than one severe wear rate occurs and modulus of elasticity is high. On the other hand, when the value of H_p to H_d is greater than one lower wear rate and modulus of elasticity after 600 m distance were obtained. According to the SEM micrograph and surface topography, it may be established $H_p/H_d = 0.5$ as a cut-off limit or critical value (point C) at which the particles failed to penetrate the NiCrBSi coating surface, and the wear regime transitioned from purely grooving to an intending (tumbling) wear regime. That is, if the hardness of the debris particles exceeds the hardness of NiCrBSi

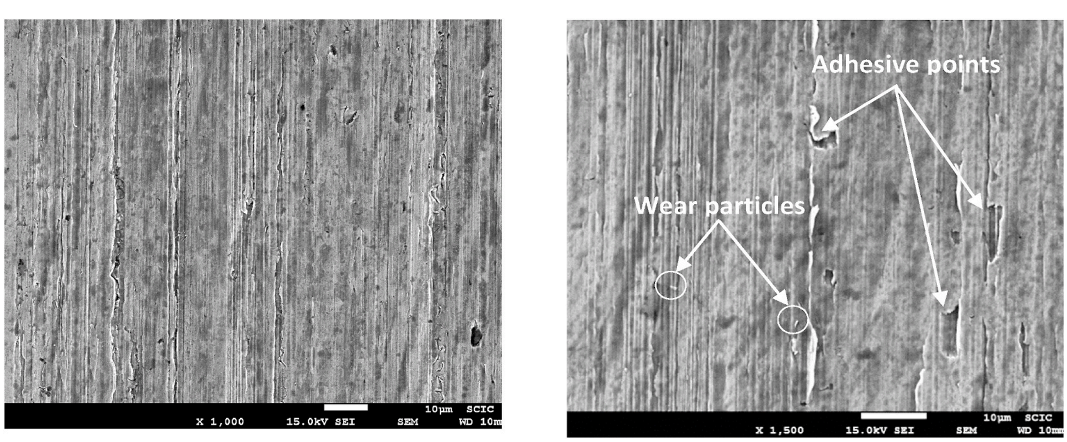

Fig. 11. Different magnification SEM images of the worn surface of NiCrBSi pin coating with solely oil after 600 m test distance.

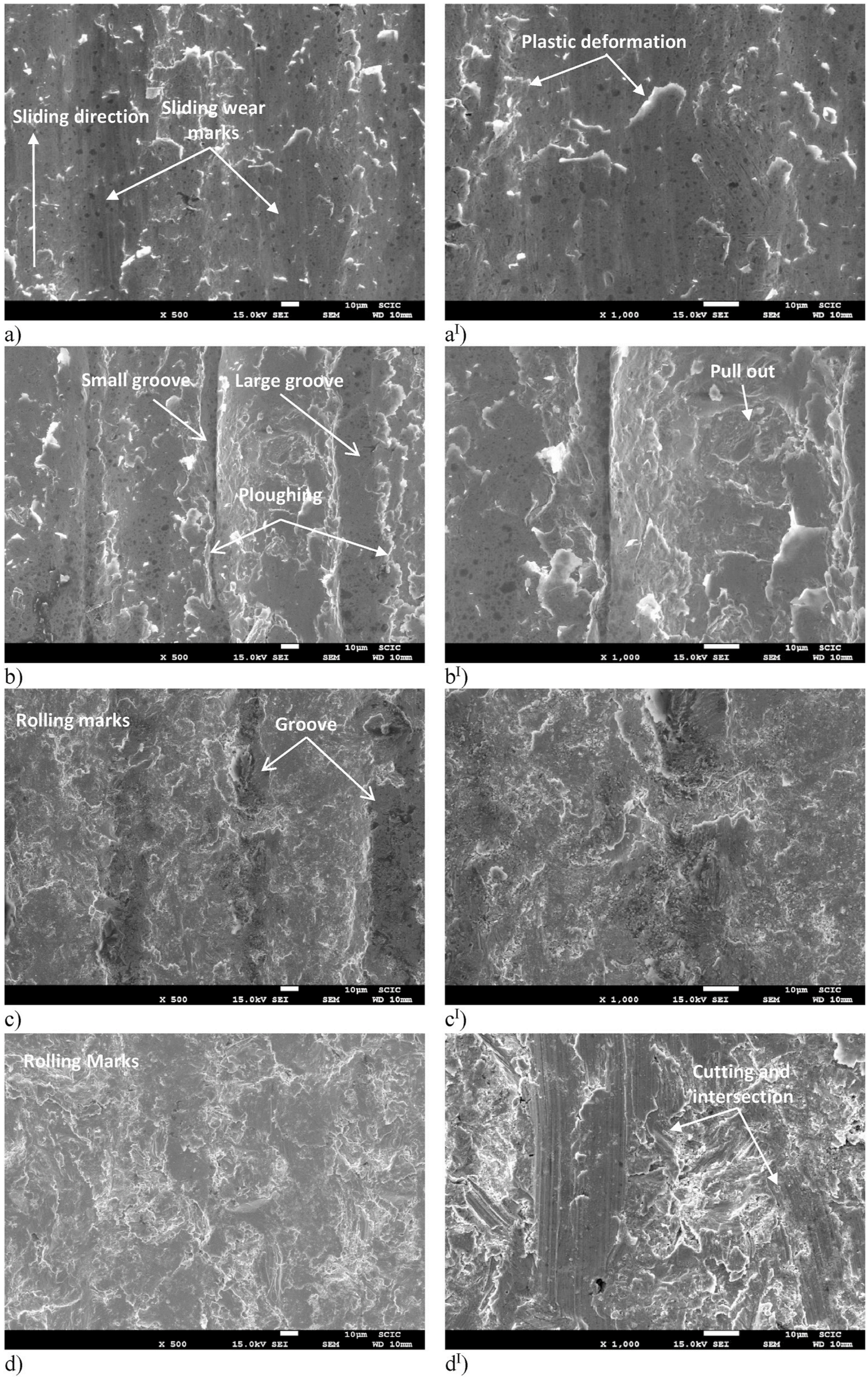

Fig. 12. SEM images of worn surface after friction of NiCrBSi specimens with different debris hardness ratio at various magnification.

coatings by a factor of 0.5, the particles could roll or slide along the surface without embedding into the surface of the NiCrBSi coatings. Consequently, the abrasive particles would no longer slide against the surface of the coating, and the wear mechanism would transition from a grooving to a rolling wear.

Additionally, wear rate versus modulus of elasticity and hardness ratio H_p/H_d relationship for NiCrBSi pin coatings shows that wear rate and modulus of elasticity are largely governed by the Hardness ratio. The increase in wear rate of NiCrBSi coating depends on the hard abrasive particles which have become embedded in a soft surface and cause more severe wear. Alternatively, a hard sharp edge or a hard debris may penetrate the softer surface of NiCrBSi coating. While the

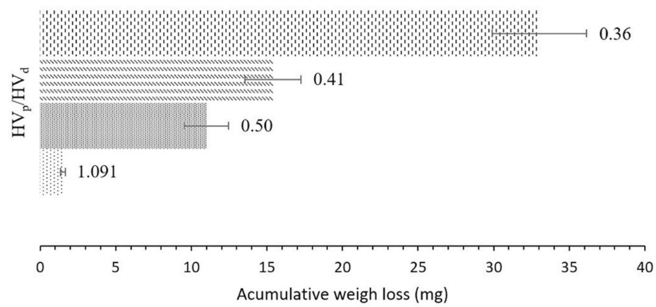

Fig. 13. Influence of hardness ratio on accumulative mass loss after 600 m of sliding distance.

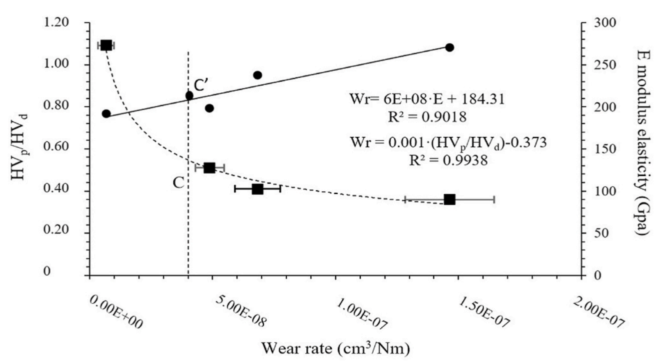

Fig. 14. Measured variation of the accumulative wear rate and modulus of elasticity of NiCrBSi coating pins, after 600 m distance as a function of hardness ratio H_p/H_d.

increase in the modulus of elasticity is mainly due to work-hardening produces during wear process. It can be observed that increasing the hardness ratio from 0.36 to 0.41 (13.8%) increases the wear rate of NiCrBSi coating (53.33%) and modulus of elasticity (12.20%), from 0.41 to 0.5 increases the wear rate about (28.57%) and modulus of elasticity (16.51) and finally from 0.5 to 1.091 increases the wear rates (86.36%) and modulus of elasticity (3.28%).

The dependence of the wear mechanism on load and abrasive concentration can be explained by an adaptation of the Williams and Hyncica [50] model. This model shows that abrasive particle between two surfaces undergoes a transition from grooving to rolling at critical value of D/h where D is the debris particle major axis and h is the separation of surfaces. In their work the separation h was determined by hydrodynamic lubrication conditions; in our case, Fig. 15 [7], the surfaces are not supported by a significant hydrodynamic pressure, and so the separation is determined principally by the applied load and hardness ratio H_p/H_d, considering that the concentration of particles is keeping constant.

Fig. 16 shows the optical microscopy of the worn surface of the counterpart discs after the wear tests using: lubricant oil + NiCrBSi (10.1%Cr) ($H_p/H_d = 1.091$), lubricant oil + NiCrBSi (15.25%Cr) ($H_p/H_d = 0.5$), Oil + NiCrBSi and (15.25%Cr)/ZSP, 60/40%) ($H_p/H_d = 0.41$) and Oil + NiCrBSi (15.25%Cr)/ZSP, 40/60%) ($H_p/H_d = 0.36$) as debris particles. A few scattered material transfer points are observed at the surface of the F-5220 disc when soft debris particles have been used, while abrasive grooves are present on the disc when the tough particles debris and NiCrBSi + ZSP mixtures were used as debris particles. The presence of small particles with different hardness between the sliding surfaces can be caused by distinguished types of wear mechanism as described below.

When particles with lower hardness (330 HV_{30gf} NiCrBSi debris particles) were used, Fig. 16a-a^{I} shows that weak signs of plastic deformation and scarring of the sliding surface in the form of adhesion are observed on the wear track and cause much less wear than the hardest particles. The oxidation of Ni-base debris particles that displaced to the higher level of bulk hardness surface face of hardened and tempered F-5220 disc, are considered to have created an effect that reduces the friction coefficient and mass loss [51,52]. When the debris with intermediate hardness NiCrBSi (15.25% Cr, 714 HV_{30gf}) were used the wear disc surface had a few amounts of scratch, Fig. 16b-b^{I}. The adherence surface film formation was less as the hardness of the debris particles increased, influencing the transition from mild to severe abrasive wear. However, when a hard abrasive debris was used (both 15.25%Cr/ZSP, 60/40%, 880 HV_{30gf}, and 15.25%Cr/ZSP, 40/60%, 1003 HV_{30gf}), the scratches formed on wear surface of the disc were deeper, with indentation marks caused by rolling abrasion, and the initial surface topography was completely altered. This can be attributed to the presence of two-body and three-body particles debris in the intermediate surface increased, and it may be due to successive fracture of brittle debris particles in the contact area (Fig. 16c-c^{I} and d-d^{I}). These particles and their contact with both NiCrBSi pin coating and counterpart hard disc increased the friction coefficient and mass loss as a function of ceramic particles content. The micro-mechanisms found in this case also corroborate those shown in the previous reported work [53] where authors proposed the possibility of fragmentation of the abrasive particles when using harder debris, such as ceramic debris, thus generating a wider particle size distribution and causing micro-rolling between grooves caused by the smaller particles.

The effect of wear on the surface roughness within the wear tracks on the discs after 600 m of distance is shown in Fig. 16 a^{II}, b^{II}, c^{II} and d^{II}. For polished surfaces ($R_a = 0.075$ μm) there was no significant change in roughness compared to NiCrBSi pin coatings. The disc surface roughness of hardened and tempered F-5220 are 5.1 times lower compared to that of NiCrBSi pin coating when soft debris NiCrBSi (10.1% Cr, 330 HV_{30gf}) is used, 6.56 times lower when tough debris NiCrBSi (15.25% Cr, 714 HV_{30gf}) is used, and the results have shown 6.54 and 4.721 times lower when both mixture debris (15.25%Cr/ZSP, 60/40%, 880 HV_{30gf}) and

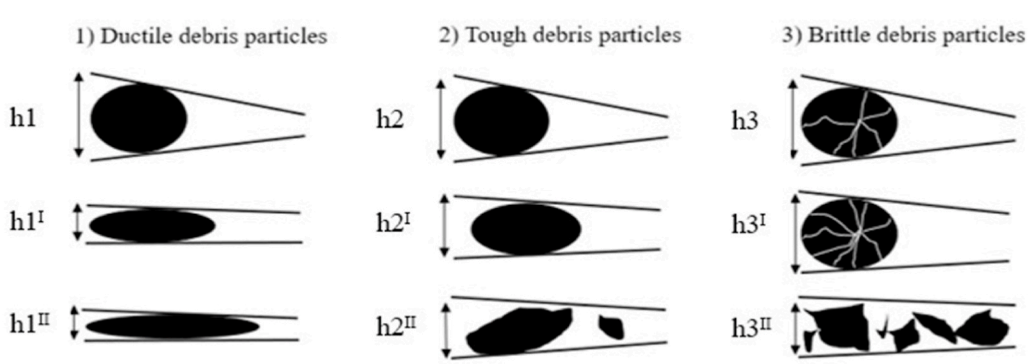

Fig. 15. Dependence of surface separation distance (h) on the particle's debris hardness.

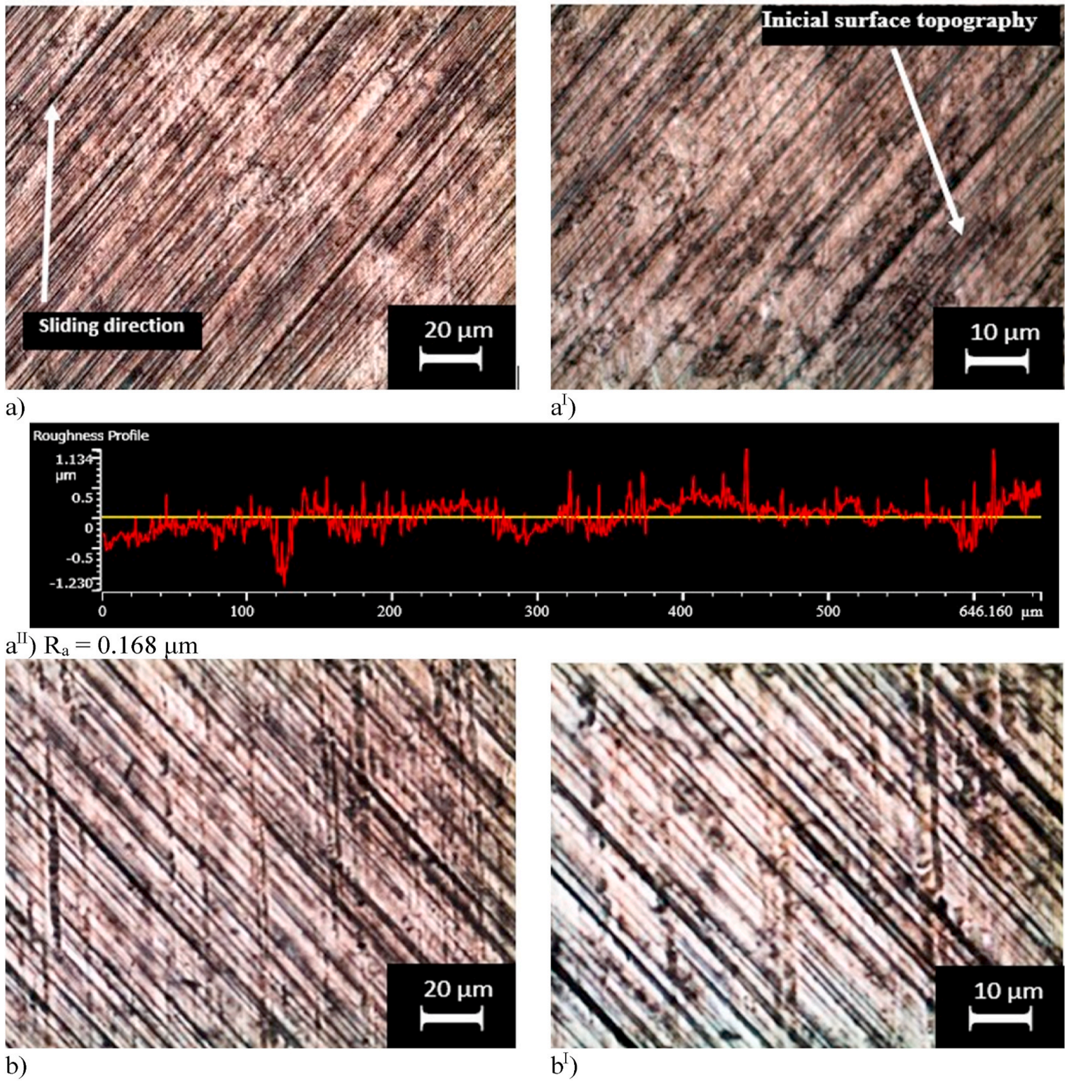

Fig. 16. Optical microscopy images and 2-D surface profile of the discs after 600 m tests performed in lubrication condition using different debris hardness: a) soft debris NiCrBSi (10.1% Cr, 330 HV_{30gf}), b) tough debris NiCrBSi (15.25% Cr, 714 HV_{30gf}), c) mixture debris (15.25%Cr)/ZSP, 60/40%, 880 HV_{30gf}) and d) (15.25% Cr)/ZSP, 40/60%, 1003 HV_{30gf}).

(15.25%Cr/ZSP, 40/60%, 1003 HV_{30gf}) had been used under the same test conditions, respectively.

4. Conclusions

The effect of hardness ratio (H_p/H_d) on friction and wear of NiCrBSi coating samples under different load and velocities was studied. Similar Stribeck curves were obtained but with different lubrication number (K_L). The transition from the higher value of lubrication number to lower regions depends on the hardness ratio. The wear rate and the modulus of elasticity increased remarkably with decrease of the hardness ratio.

In order to take into account the effect of hardness ratio (H_{pin}/H_{debris}) on the surface roughness and predict the Stribeck curve, a ratio of the hardness of tested samples was incorporated into the lubricant number Z.

The worn surface observations, using a rugosimeter and scanning electron microscope suggest that, together with the shape, size, and number of debris, the hardness ratio (H_p/H_d) must be considered when studying the tribological behavior and in the engineering design of machine components.

This research shows that the relation between the hardness ratio and final surface roughness is not linear but piecewise. We found that there exists a cut-off limit from a low to a higher friction coefficient and wear rate under mixed lubrication regime. So, a suitable selection of hardness ratio (H_{pin}/H_{debris}) when designing the components could lead to an increase in machinery availability.

The surface damage of the NiCrBSi coating depends on the coupled action of the debris hardness and lubrication regime. If there was no thick lubrication film separating the friction pairs, the harder debris particles would penetrate the NiCrBSi coating in the sliding process; therefore, the friction force would be increased.

In many industrial applications, which are exposed to abrasive conditions, it is beneficial to take into account the importance of both coating and debris hardness. As shown in the present study, tribopairs with a higher hardness ratio (H_p/H_d) of 1.091 outperform other tribopairs with lower hardness ratios. As a design parameter, determining the optimum cut-off limit or critical value ($H_p/H_d = 0.5$ in this study) for each friction pair at which the friction coefficient and the wear rate change drastically may help to better control the energy savings and material losses in each case.

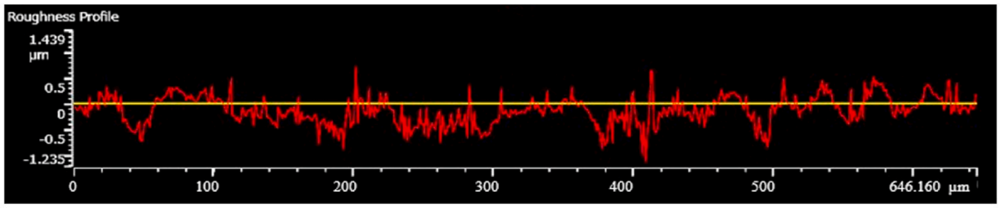

b^{II}) $R_a = 0.207$ µm

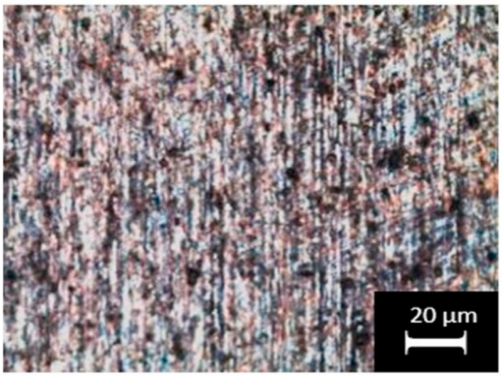

c)

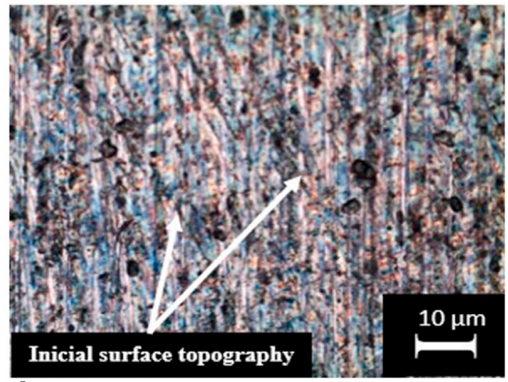

c^{I})

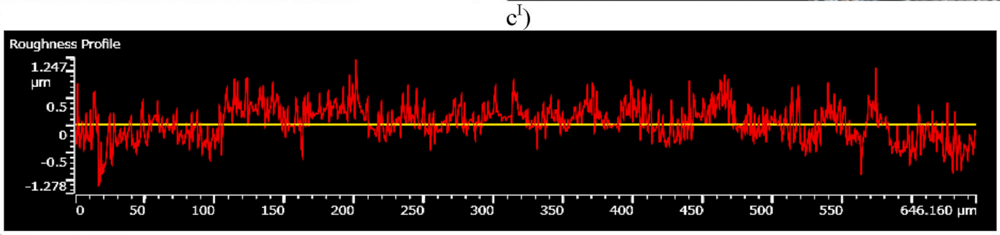

c^{II}) $R_a = 0.239$ µm

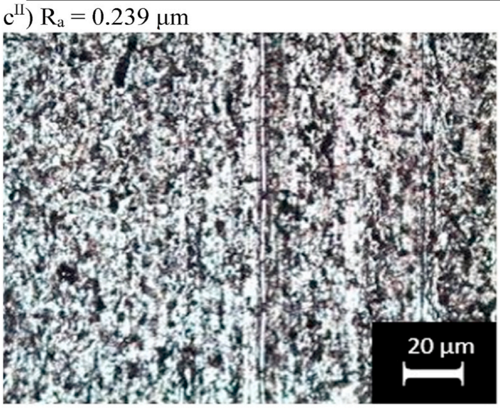

d)

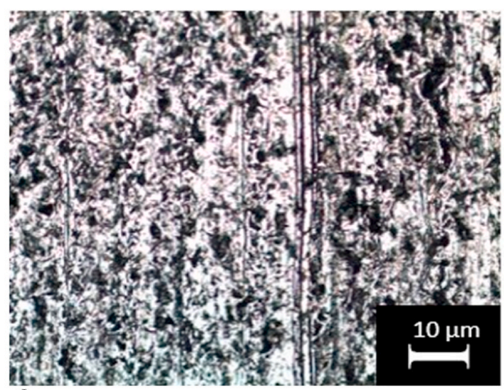

d^{I})

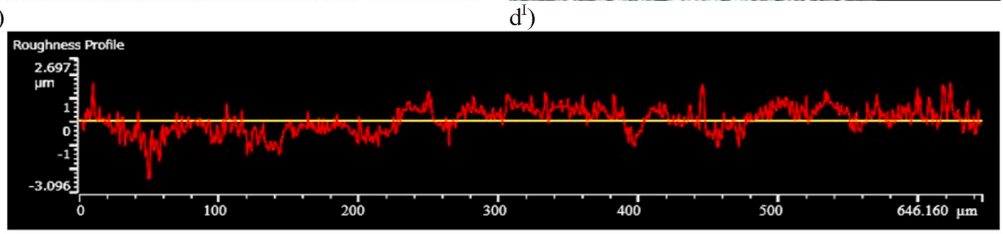

d^{II}) $R_a = 0.385$ µm

Fig. 16. (*continued*).

Declaration of competing interest

The authors declare that they have no known competing financial interests or personal relationships that could have appeared to influence the work reported in this paper.

References

[1] K.H. Gahr, Microstructure and Wear of Materials, Elsevier Science Publishers, P. O. Box 211, 1000 AE Amsterdam, The Netherlands, 1987, 1987.
[2] G.K. Nikas, A state-of-the-art review on the effects of particulate contamination and related topics in machine-element contacts, Proc. IME J. J. Eng. Tribol. 224 (5) (2010) 453–479.
[3] L. Du, J. Zhe, Parallel sensing of metallic wear debris in lubricants using under sampling data processing, Tribol. Int. 53 (2012) 28–34.
[4] A. Kontou, M. Southby, N. Morgan, H.A. Spikes, Influence of dispersant and ZDDP on soot wear, Tribol. Lett. 66 (4) (2018) 157.

[5] R.S. Dwyer-Joyce, The life cycle of a debris particle, in: Tribology and Interface Engineering Series, vol. 48, Elsevier, 2005, pp. 681–690.
[6] E. Cihan, K. Jungjohann, N. Argibay, M. Chandross, M. Dienwiebel, Effect of environment on microstructure evolution and friction of Au–Ni multilayers, Tribol. Lett. 68 (2020) 1, 30.
[7] G.K. Nikas, A state-of-the-art review on the effects of particulate contamination and related topics in machine-element contacts, Proc. IME J. J. Eng. Tribol. 224 (5) (2010) 453–479. https://doi:10.1243/13506501JET752.
[8] H.O.N.G. Wei, C.A.I. Wenjian, Shaoping Wang, M. Mileta, TOMOVIC, Mechanical wear debris feature, detection, and diagnosis: a review, Chin. J. Aeronaut. 31 (5) (2018) 867–882, https://doi.org/10.1016/j.cja.2017.11.016.
[9] N. Dörr, A. Agocs, C. Besser, A. Ristić, M. Frauscher, Engine oils in the field: a comprehensive chemical assessment of engine oil degradation in a passenger car, Tribol. Lett. 67 (3) (2019) 68.
[10] O. Barrau, C. Boher, R. Gras, F. Rezai-Aria, Wear mechanisms and wear rate in a high temperature dry friction of AISI H11 tool steel: influence of debris circulation, Wear 263 (2007) 160–168. https://doi:10.1016/j.wear.2006.12.032.
[11] A. Ronen, S. Malkin, K. Loewy, Wear of dynamically loaded hydrodynamic bearings by contaminant particles, J. of Lubrication Tech. 102 (4) (1980) 452–458, https://doi.org/10.1115/1.3251580.
[12] A. Ronen, S. Maikin, Investigation of friction and wear of dynamically loaded hydrodynamic bearings with abrasive contaminants, Journal of Lubrication Technology 105 (1983) 559–567.
[13] E.A. Khorshid, A.M. Nawwar, A review of the effect of sand dust and filtration on automobile engine wear, Wear 141 (2) (1991) 349–371.
[14] M.R. Sari, A. Haiahem, L. Flamand, Effect of lubricant contamination on gear wear, Tribol. Lett. 27 (1) (2007) 119–126.
[15] T. Akagaki, M. Nakamura, T. Monzen, M. Kawabata, Analysis of the behaviour of rolling bearings in contaminated oil using some condition monitoring techniques, Proc. IME J. J. Eng. Tribol. 220 (5) (2006) 447–453.
[16] F. Ville, D. Nelias, Early fatigue failure due to dents in EHL contacts, Tribol. Trans. 42 (4) (1999) 795–800.
[17] R. Nilsson, U. Olofsson, K. Sundvall, Filtration and coating effects on self-generated particle wear in boundary lubricated roller bearings, Tribol. Int. 38 (2) (2005) 145–150.
[18] M. Moon, How clean are your lubricants? Trends Food Sci. Technol. 18 (2007) S74–S79, https://doi.org/10.1016/j.tifs.2006.11.002.
[19] P.S.G. Cross a, G. Limbert, D. Stewart, R.J.K. Wood, A Multiscale Finite Element Model of Sliding Wear for Cobalt-Chromium Undergoing Ratcheting Wear, vols. 462–463, 2020, p. 203482, https://doi.org/10.1016/j.wear.2020.203482.
[20] J.C. Hamer, R.S. Sayles, E. Ioannides, Particle deformation and counter face damage when relatively soft particles are squashed between hard anvils, Tribol. Trans. 32 (3) (1989) 281–288.
[21] Y.S. Kang, F. Sadeghi, M.R. Hoeprich, A finite element model for spherical debris denting in heavily loaded contacts, ASME Journal of Tribology 126 (1) (2004) 71–80.
[22] E. Antaluca, D. Nélias, Contact fatigue analysis of a dented surface in a dry elastic–plastic circular point contact, Tribol. Lett. 29 (2) (2008) 139–153.
[23] F. Ville, D. Nelias, Influence of the nature and size of solid particles on the indentation features in EHL contacts, in: Tribology Series, vol. 34, Elsevier, 1998, pp. 399–409.
[24] D.G. Grieve, R.S. Dwyer-Joyce, J.H. Beynon, Abrasive wear of railway track by solid contaminants, Proc. Inst. Mech. Eng. - Part F J. Rail Rapid Transit 215 (3) (2001) 193–205.
[25] R. Nilsson, R.S. Dwyer-Joyce, U. Olofsson, Abrasive wear of rolling bearings by lubricant borne particles, Proc. IME J. J. Eng. Tribol. 220 (5) (2006) 429–439.
[26] A. Kontoua, M. Southby, H.A. Spikes, Effect of steel hardness on soot wear, Wear 390–391 (2017) 236–245, https://doi.org/10.1016/j.wear.2017.07.020.
[27] K.A. Habib, D.L. Cano, J.A. Heredia, A. Vicente-Escuder, Effect of debris size on the tribological performance of thermally sprayed coatings, Tribol. Int. 143 (2020) 106025.
[28] M.X. Shen, B. Li, D.H. Ji, G.Y. Xiong, L.Z. Zhao, J. Zhang, Z.N. Zhang, Effect of particle size on tribological properties of rubber/steel seal pairs under contaminated water lubrication conditions, Tribol. Lett. 68 (2020) 1, 40.
[29] D.A. Rigney, The roles of hardness in the sliding behavior of materials, Wear 175 (1–2) (1994) 63–69.
[30] P.J. Firkins, J.L. Tipper, E. Ingham, M.H. Stone, R. Farrar, J. Fisher, A novel low wearing differential hardness, ceramic-on-metal hip joint prosthesis, J. Biomech. 34 (10) (2001) 1291–1298.
[31] G. Straffelini, F. Bonollo, A. Molinari, A. Tiziani, Influence of matrix hardness on the dry sliding behaviour of 20 vol.% Al_2O_3-particulate-reinforced 6061 Al metal matrix composite, Wear 211 (2) (1997) 192–197.
[32] C. Trevisiol, A. Jourani, S. Bouvier, Effect of hardness, microstructure, normal load and abrasive size on friction and on wear behaviour of 35NCD16 steel, Wear 388 (2017) 101–111.
[33] J.M. Miguel, J.M. Guilemany, S. Vizcaino, Tribological study of NiCrBSi coating obtained by different processes, Tribol. Int. 36 (3) (2003) 181–187.
[34] Bobzin, F. Ernst, J. Zwick, T. Schlaefer, D. Cook, K. Nassenstein, A. Schwenk, F. Schreiber, T. Wenz, G. Flores, M. Hahn, Coating bores of light metal engine blocks with a nanocomposite material using the plasma transferred wire arc thermal spray process, J. Therm. Spray Technol. 17 (3) (2008) 344–351.
[35] Q. Ming, L.C. Lim, Z.D. Chen, Laser cladding of nickel-based hardfacing alloys, Surf. Coating. Technol. 106 (2–3) (1998) 174–182.
[36] H.J. Kim, S.Y. Hwang, C.H. Lee, P. Juvanon, Assessment of wear performance of flame sprayed and fused Ni-based coatings, Surf. Coating. Technol. 172 (2–3) (2003) 262–269.
[37] A. Stathis, D. Koulocheris, T. Costopoulos, V. Spitas, The impact of particle contaminants' hardness on the wear mechanism of rolling element bearings, Int. J. 1 (1) (2014) 10–19.
[38] D.J. Schipper, P.H. Vroegop, A.W.J. De Gee, Prediction of lubrication regimes of concentrated contacts, Lubric. Sci. 3 (3) (1991) 191–200.
[39] I. Mukchortov, E. Zadorozhnaya, E. Polyacko, Transitional friction regime modeling under boundary lubrication conditions, Procedia Engineering 206 (2017) 725–733.
[40] A. Moshkovich, V. Perfilyev, D. Gorni, I. Lapsker, L. Rapoport, The effect of Cu grain size on transition from EHL to BL regime (Stribeck curve), Wear 271 (2011) 9–10, 1726-1732, http://doi:10.1016/j.wear.2010.12.052.
[41] Aleks Vrček, Hultqvist Tobias, Johannesson Tomas, Pär Marklund, Roland Larsson, Micro-pitting and wear characterization for different rolling bearing steels: effect of hardness and heat treatments, Wear (2020) 458–459, 203404.
[42] B.J. Hamrock, D. Dowson, Isothermal elastohydrodynamic lubrication of point contacts Part 1-theoretical formulation the, J. Lubr. Technol. 99 (2) (1976) 223–228.
[43] L. Calabri, N. Pugno, C. Menozzi, S. Valeri, AFM nanoindentation: tip shape and tip radius of curvature effect on the hardness measurement, J. Phys. Condens. Matter 20 (2008) 47, 474208.
[44] V.M. Masterson, X. Cao, Evaluating particle hardness of pharmaceutical solids using AFM nanoindentation, Int. J. Pharm. 362 (1–2) (2008) 163–171.
[45] I. Hutchings, P. Shipway, Tribology: Friction and Wear of Engineering Materials, second ed., Butterworth-Heinemann, 2017.
[46] K.A. Habib, D.L. Cano, José Antonio Heredia, J.Serrano Mira, Effect of post-coating technique on microstructure, microhardness and themixed lubrication regime parameters of thermally-sprayed NiCrBSi coatings, Surf. Coating. Technol. 358 (2019) 824–832, https://doi.org/10.1016/j.surfcoat.2018.12.004.
[47] M.A. Mekich, M.B. de Rooij, T. Mishr, D.T.A. Matthews, L. Jacobs, D.J. Schipper, Study of Wear Particles Formation at Single Asperity Contact: an Experimental and Numerical Approach, vols. 470–471, 2021, p. 203644, https://doi.org/10.1016/j.wear.2021.203644, 5 April.
[48] A. Fischer, W. Dudzinski, B. Gleising, P. Stemmer, Analyzing mild- and ultra-mild sliding wear of metallic materials by transmission electron microscopy, in: M. Dienwiebel, M.-I. de Barros (Eds.), Triboanalytics, Springer, Germany, Springer, Berlin, Germany, 2018, pp. 29–59.
[49] F. Brownlie, T. Hodgkiess, A.M. Galloway, A. Pearson, Experimental investigation of engineering materials under repetitive impact with slurry conditions, Tribol. Lett. 69 (1) (2021) 1–15.
[50] J.A. Williams, A.M. Hyncica, Mechanisms of abrasive wear in lubricated contact, Wear 152 (No. 1) (1994) 57–74.
[51] C.A.I. Bin, Y.F. Tan, T.A.N. Hua, Q.F. Jing, Z.W. Zhang, Tribological behavior and mechanism of NiCrBSi–Y2O3 composite coatings, Trans. Nonferrous Metals Soc. China 23 (7) (2013) 2002–2010.
[52] V. Stoica, R. Ahmed, T. Itsukaichi, S. Tobe, Sliding wear evaluation of hot isostatically pressed (HIPed) thermal spray cermet coatings, Wear 257 (11) (2004) 1103–1124, https://doi.org/10.1016/j.wear.2004.07.016.
[53] M.A. N Ardila, H.I. Costa, J.D.B. De Mello, Influence of the ball material on friction and wear in microabrasion tests, Wear (2020) 450–451.